AIAA 97-0435

Treatments of Stiff Source Terms in Conservation Laws by the Method of Space-Time Conservation Element and Solution Element

Sheng-Tao Yu
NYMA Technology, Inc.
NASA Lewis Research Center
Cleveland, OH

Sin-Chung Chang
NASA Lewis Research Center
Cleveland, OH

35th Aerospace Sciences Meeting & Exhibit
January 6-10, 1997 / Reno, NV

Treatments of Stiff Source Terms in Conservation Laws by the Method of Space-Time Conservation Element/Solution Element

Sheng-Tao Yu*
NYMA Technology, Inc.
NASA Lewis Research Center
Cleveland, OH

Sin-Chung Chang†
NASA Lewis Research Center
Cleveland, OH

Abstract

In this paper, we report an extension of the CE/SE method for simulating conservation laws with stiff source terms. In contrast to the modern upwind schemes, the approach here does not use the reconstruction and Riemann solver as the building blocks. Therefore, the logic is considerably simpler. The treatment is based on a volumetric integration of the source terms over space-time conservation elements such that the source terms are treated directly as an integral part of the overall space-time flux balance. Two space-time geometries are reported: (1) the rhombic conservation elements, and (2) the rectangular conservation elements. The method of rhombic element can be used to treat the non-stiff source terms. The method of rectangular elements is suited for stiff source terms. Both methods result in locally implicit formulations and Newton's method is used to solve the equations. Four examples are reported in the paper: (1) standing normal shock in a quasi-one-dimensional flow, (2) LeVeque and Yee's test case using a cubic function of the unknown as the source term; (3) a shock tube in a constant-temperature bath, and (4) the ZND detonation waves.

1 Introduction

Recently, Chang and coworkers [1-10] reported a new framework for the numerical solution of conservation laws, namely, the Method of Space-Time Conservation Element and Solution Element, or the CE/SE method for short. This method is distinguished by the simplicity of its conceptual basis – a unified treatment of flux conservation in space and time. In describing the method, Chang took the most direct approach, i.e., starting from the basic integral equations, the algebraic details and the mathematical analyses were presented in a systematic way. All informations needed to implement a computer software were included. That approach made it clear that the CE/SE method was developed from fundamentals. It is not an incremental improvement of a previously existing method.

The original CE/SE scheme for solving the one-dimensional scalar convection equation [1,6,7] is *explicit, non-dissipative* (or neutrally stable), and involves only *two time levels.* To assist the reader in getting a flavor of the CE/SE Euler schemes, we provide the following remarks: (i) For isentropic flows, the CE/SE method is neutrally stable for CFL ≤ 1, and it can march forward and backward in time. (ii) A staggering spatial mesh, which zigzags as time evolves, is employed, such that flow information at each interface separating adjacent CEs can be evaluated without using a Riemann solver. (iii) The inner structure of the flow solution is not calculated through a reconstruction procedure. In-

*Senior Engineer, E-mail: styu@lerc.nasa.gov.
†Senior Scientist, E-mail: vvscc@noboo.lerc.nasa.gov.

stead, the gradients of flow variables are treated as independent unknowns, and they are not influenced by the flow properties in neighboring elements at the same time level. This is in full compliance with the flow physics of the initial value problem. (iv) For flows in multiple spatial dimensions, no directional splitting is employed. The two and three-dimensional spatial meshes employed by the CE/SE method are built from triangles and tetrahedrons. Note that triangles and tetrahedrons are also the simplest building blocks for two and three-dimensional unstructured meshes.

Computer programs based on the CE/SE method have been developed for calculating flows in one and two spatial dimensions. Numerous results were obtained [11-19]. In addition, Scott [20-24] has developed an implicit steady-state version of the space-time method for simulating steady-state incompressible flows.

In the present paper, we extend the CE/SE method to solve the conservation laws with source terms. The extension of the CE/SE method is illustrated by focusing on its space-time discretization. In particular, the role of the source term and its numerical treatment can be grasped by a simple delineation of the inherent space-time geometries of the present method.

In this introduction, we shall first illustrate the idea of the unified treatment of space and time in the integral equations for the flux balance. As a contrast to the conventional finite-volume methods, this unified treatment provides a lucid picture for the source-term effect. For the background material of the present work, we shall also briefly review the current numerical methods for solving conservation laws with stiff source terms.

1.1 The Finite-Volume Methods

Conventionally, the space-time flux balance of conservation laws has been mathematically described by formulations either in a Lagrangian frame or in an Eulerian frame. Formulations in these two different coordinate frames can be bridged by Reynold's transport theorem [25]:

$$\frac{d}{dt}\int_{V_t} u dV_t = \int_{V_t} \frac{\partial u}{\partial t} dV_t + \int_{S(V_t)} u\vec{v}\cdot d\vec{s}, \quad (1.1)$$

where u is the density of a conserved property, V_t denotes the spatial volume of integration at time t, $S(V_t)$ is the surface of V_t, and $d\vec{s} = d\sigma\,\vec{n}$ with $d\sigma$ and $\vec{n}$, respectively, being the area and the outward unit normal vector of a surface element on $S(V_t)$. The points inside V_t move with velocity $\vec{v}$, generating the motion of the volume. The left hand side of Eq. (1.1) is based on the Lagrangian frame; the right hand side is based on the Eulerian frame. Note that space and time are treated in different manners.

Consider a scalar convection equation with a source term,

$$u_t + \vec{\nabla}\cdot\vec{f} = p, \quad (1.2)$$

where p is the density of the source, and and $\vec{f} = u\vec{v}$ with $\vec{v}$ being the constant convection velocity. An integral counterpart to Eq. (1.2) in a Lagrangian frame is

$$\frac{d}{dt}\int_{V_t} u dV_t = \int_{V_t} p dV_t. \quad (1.3)$$

By using Reynold's transport theorem, we also have

$$\int_{V_t} \frac{\partial u}{\partial t} dV_t + \int_{S(V_t)} \vec{f}\cdot d\vec{s} = \int_{V_t} p dV_t. \quad (1.4)$$

To solve Eq. (1.4), the conventional finite-volume methods [26] reformulate the equation based on *a fixed spatial domain*, i.e.,

$$\frac{\partial}{\partial t}\int_{V} u dV = -\int_{S(V)} \vec{f}\cdot d\vec{s} + \int_{V} p dV. \quad (1.5)$$

As such, the conservation laws state that the rate of change of the total amount of a substance contained in *a fixed spatial domain* V is equal to the combination of the following two effects: (i) the flux of that substance across the boundary of V, i.e., $S(V)$, and (ii) the integration of the source term over the fixed spatial domain. The conventional finite-volume methods concentrate on the

evaluation of the right hand side of Eq. (1.5). The left hand side of Eq. (1.5) is usually discretized by a finite-difference method. e.g., the Runge-Kutta methods. In light of the above two effects, the fractional-step (or splitting) methods resort to strong measures of numerically segregating the two effects and treating them in a sequential fashion.

Alternatively, one could integrate Eq. (1.5) with respect to time from t_1 to t_2, i.e.,

$$\int_V u dV \Big|_{t_1}^{t_2} = \int_{t_1}^{t_2} dt \left(- \int_{S(V)} \vec{f} \cdot d\vec{s} + \int_V p dV \right). \tag{1.6}$$

As compared to Eq. (1.5), Eq. (1.6) depicts a clearer picture of the space-time flux balance.

As shown in Fig. 1.1(a), due to *the fixed spatial domain*, the shape of the space-time CEs in one spatial dimension must be rectangular. In addition, these elements must stack up exactly on top of each other in the time-direction, i.e., no staggering of CEs in time is allowed. For equations in two spatial dimensions, as depicted in Fig. 1.1(b), a conservation element is a uniform-cross-section cylinder in space-time, and again no staggering in time is allowed. This arrangement results in vertical interfaces extended in the direction of time evolution between adjacent CEs. Across these interfaces, flow information travels in both directions. Therefore, upwind bias (or a Riemann solver) becomes necessary in calculating the interfacial flux.

1.2 The Integral Equation of the CE/SE Method

In the present method, as a contrast to Reynold's transport theorem Eq. (1.1), space and time are treated in a unified manner. Consider a set of M coupled convection equations in one spatial dimension:

$$\mathbf{U}_t + \mathbf{F}_x = \mathbf{P}, \quad \mathbf{U} \in \mathbf{R}^M, \tag{1.7}$$

where $\mathbf{U}$ is the unknown vector, $\mathbf{F}$ is the spatial flux vector, and $\mathbf{P}$ is the source term vector. As shown in Fig. 1.2, let $x_1 = x$, and $x_2 = t$ be the coordinates of a two-dimensional Euclidean space E_2, and all mathematical operations, such as div, curl, and grad, can be carried out as if E_2 was an ordinary two-dimensional Euclidean space. Thus, Eq. (1.7) can be expressed as M scalar equations:

$$\nabla \cdot \vec{\mathbf{h}}_m = p_m \quad m = 1, 2, \ldots, M \tag{1.8}$$

where $\vec{\mathbf{h}}_m = (f_m, u_m)$, and f_m, u_m, and p_m are the mth components of $\mathbf{F}$, $\mathbf{U}$, and $\mathbf{P}$, respectively. Equation (1.8) is valid everywhere in E_2 for continuous flow solutions.

For solutions with discontinuities, an integral counterpart to Eq. (1.8) must be employed:

$$\oint_{S(R)} \vec{\mathbf{h}}_m \cdot d\vec{s} = \int_R p_m dR, \quad m = 1, 2, \ldots, M \tag{1.9}$$

where $S(R)$ is the boundary of a space-time region R, and $d\vec{s}$ represents a surface element of $S(R)$. Note that Eq. (1.9) is more fundamental than Eq. (1.8), and can be derived directly from the space-time flux balance. Equation (1.8), on the other hand, is valid only for smooth solutions, and can be derived from Eq. (1.9) using Gauss' divergence theorem.

Equation (1.9) states that the total space-time flux of $\vec{\mathbf{h}}_m$ leaving R through its boundary is equal to the integration of the source term p_m over the space-time region R. As a contrast to the formulations used in the conventional finite-volume methods, i.e., Eqs. (1.5) and (1.6), the present formulation does not impose any constraint on the shape of the CEs in the space-time domain. This is the crucial difference that, at the conceptual level, separates the CE/SE method from the conventional finite-volume methods.

We remark that the conventional space-time integration Eq. (1.6) is a special case of Eq. (1.9). For flows in one spatial dimension using *a fixed spatial domain* for CEs, the left hand side of Eq. (1.9) can be converted into a line integration, i.e.,

$$\oint_{S(R)} \vec{\mathbf{h}}_m \cdot d\vec{s} = \oint_{S(R)}^{c.c.} (f_m dt - u_m dx),$$

$$m = 1, 2, \ldots, M \qquad (1.10)$$

where *c.c.* indicates that the line integration is carried out in the counterclockwise direction. Facilitated by Eq. (1.10), one can show that Eq. (1.9) is equivalent to Eq. (1.6) in this special condition. Moreover, if one assumed that the temporal evolution of U is smooth, which of course is not true in the case of a moving shock, one can derive Eq. (1.5) by differentiating both sides of Eq. (1.6) with respect to time.

1.3 Treatments of Stiff Source Terms

Convection equations with source terms are commonly referred to as relaxation systems, and they are commonplace in various physical problems. In particular, we are interested in solving the transport equations for combustion systems using finite-rate kinetics. The present paper is a stepping stone towards the development of a comprehensive computer program for simulating combustion dynamics.

As an example, consider the following relaxation system, in which only one time scale, i.e., ϵ, is associated with the M source terms:

$$\mathbf{U}_t + \mathbf{F}_x = \frac{1}{\epsilon}\mathbf{P}, \quad \mathbf{U} \in R^M. \qquad (1.11)$$

When $\epsilon \to 0$, the time scale of the source term is much smaller than the characteristic time scale of the hyperbolic system, and the equation set is stiff.

We remark that the disparities between the time scales for the convectional transportation and the time scale of the source terms, such as that in Eq. (1.11), is not the sole source of stiffness in a more general equation set. In modeling a combustion system by a finite-rate chemistry, the stiffness of the source terms in the species equations depends on the order of the magnitude of the reaction rate constants, which could easily range from 10^3 to 10^{30} for the combustion of a typical hydrocarbon fuel. In simulating the chemical reactions in a well-stirred reactor, in which fluid mechanics is not of interest, the disparities among reaction rate constants account for the classical stiffness problem. In what follows, we review some of the numerical treatments to the convection equations with stiff source terms.

Colella et al. [27] applied Godunov's method to solve the equations of detonation waves. In their approach, the flow equations were coupled with a single species equation, in which a source term for an irreversible finite-rate reaction step was included. A fractional-step finite-difference method was used to treat the source term. They studied the one-dimensional detonation waves with increasing stiffness of the source term. At some point, reaction zone was underresolved due to insufficient resolution of the time step and mesh size, and the numerical solution bifurcated to a non-physical reactive wave followed by a fluid dynamic shock. The spurious reaction wave moved at a false rate of one grid node per time step. Their study exposed the difficulties of using the modern upwind schemes in solving the hyperbolic systems with stiff source terms.

LeVeque and Yee [28] proposed to develop robust numerical methods that allow larger time steps without fully resolving the time and space scales associated with the source terms, and they suggested the following requirements: (i) The solutions of hyperbolic systems must be numerically stable. (ii) Shocks and contact discontinuity must be sharply resolved and a second-order accuracy is required in smooth region. (iii) the magnitude of the jump and the shock location predicted by the scheme should be correct. Based on these requirements, they experimented on a scalar equation with a source term using various splitting methods.

Pember [29, 30] suggested that the subcharacteristics by Liu [31] and the equilibrium limit of relaxation systems by Whitham [32] could be employed as the guiding principle to analyze numerical treatments to convection equations with stiff source terms. In many cases, an equilibrium counterpart to the relaxation sys-

tem, Eq. (1.11), can be found:

$$\mathbf{u}_t + \mathbf{f}(\mathbf{u})_x = 0, \qquad \mathbf{u} \in R^N, \tag{1.12}$$

where $N < M$. Note that there is no source term in this equilibrium system. To ensure the existence of this equilibrium counterpart, a sub-characteristic condition, which is an inequality relationship between the eigenvalues of the relaxation system and that of the equilibrium system, must be satisfied. For such relaxation systems, the solution asymptotically approaches the equilibrium solution as $\epsilon \to 0$. Based on these theorems, Pember experimented on a second-order upwind scheme with a semi-implicit treatment to the source terms.

Based on the logic of shooting for the equilibrium state of a relaxation system, Jin [33] incorporated the physical asymptotics of the relaxation system into the numerical scheme in a semi-discrete manner. The semi-discrete equation was then extended using a Runge-Kutta method coupled with a stiff ODE solver. Jin's method provided the first successful numerical solution to Euler equations with stiff source terms. The method, however, was complex and required some knowledge of the asymptotics of the relaxation system. In addition, the incorporation of the asymptotics and the use the Runge-Kutta method were based on the assumption that the temporal evolution of the flow properties is smooth. For unsteady flow solutions with discontinuities, e.g., a moving shock waves, further investigation is needed about the asymptotics of the relaxation system.

Roe and Arora [34, 35] developed an explicit, characteristic-based method for solving convection equations with source terms. The method was based on tracing the dispersive characteristic waves caused by the source terms. The method was accurate for non-stiff source terms. As the stiffness becomes severe, their method was stable and provided reasonable solutions. It is difficult, however, to extend this method to solve the relaxation systems in multiple spatial dimensions. Note that directional splitting is commonly used in modern upwind schemes because there is no known analytical solution to the Riemann problem in multiple spatial dimensions. Source terms, however, have no direction, and it will be difficult to construct a characteristic-based method for the relaxation systems in multiple spatial dimensions.

One could also resort to the option of locally resolving the time and space scales associated with the source terms. In this regard, the adaptive mesh refinement method [36], the sub-cell resolution method [37], and the method of adaptive refinement coupled with the front tracking [38, 39] could be used to locally resolve the flow solution. In many cases, however, the amount of refinement needed to fully resolve the space and time scales is beyond the currently available resources. Nevertheless, these adaptive refinement methods could be used in conjunction with a successful treatment to the stiff source terms.

In the present work, we are not interested in fully resolving the time and space scales of stiff source terms. Instead, we intend to develop a robust numerical method in which the stability constraint is solely based on the CFL number condition. As a contrast to Jin's splitting method and Roe and Arora's characteristic method, the present approach is based on local and global space-time flux balance. As such, the source-term effects can be visualized through the space-time geometries of the conservation elements.

The remainder of the paper is organized as follows. In Section 2, we present the extended CE/SE method for treating convection equations with source terms. In Section 3, we present the numerical examples calculated by the extended CE/SE methods. We then offer several concluding remarks.

2 The CE/SE Methods for Source Terms

In this section, we discuss the extension of the CE/SE method to solve the relaxation systems

with M unknowns in one spatial dimension. First, the preliminaries of the space-time discretization in the CE/SE method will be illustrated. We then present the method of rhombic elements for treating the non-stiff source terms, and the method of rectangular elements for the stiff source terms.

2.1 Preliminaries

In Fig. 2.1, we show the nodal locations where the unknowns are stored. The space and time intervals between neighboring nodes are denoted by $\Delta x/2$ and $\Delta t/2$. There is a Solution Element (SE) associated with each node (j,n). Let the SE(j,n) be the interior of the space-time region bounded by a dashed line as depicted in Fig. 2.2. For convection equations with non-stiff source terms, rhombic elements are of interest. Inside a SE, the flow properties are assumed continuous, and the distribution of flow properties is discretized by a first-order Taylor expansion of x and t with respect to the mesh node (x_j,t^n); i.e., the error is second order in Δx and Δt. Between SEs, discontinuities are allowed. The union of all SEs covers the whole space-time domain, such that discrete flow properties can be calculated at all space-time locations of interest.

To proceed, let $\mathbf{U}^*$ and $\mathbf{F}^*$ be the discretized counterparts to $\mathbf{U}$ and $\mathbf{F}$. Since a linear distribution $\mathbf{U}^*$ and $\mathbf{F}^*$ is assumed for any (x,t) in SE(j,n), we have

$$\begin{aligned}\mathbf{U}^*(x,t;j,n) &= \mathbf{U}_j^n + (\mathbf{U}_x)_j^n(x-x_j) \\ &\quad +(\mathbf{U}_t)_j^n(t-t^n), \qquad (2.1)\\ \mathbf{F}^*(x,t;j,n) &= (\mathbf{F})_j^n + (\mathbf{F}_x)_j^n(x-x_j) \\ &\quad +(\mathbf{F}_t)_j^n(t-t^n), \qquad (2.2)\end{aligned}$$

where $\mathbf{U}_j^n$ and $(\mathbf{U}_x)_j^n$ represent the numerical approximation to $\mathbf{U}$ and $\mathbf{U}_x$ at (x_j,t^n) and they are the primary unknowns in the present scheme. As will be illustrated in the following section, $(\mathbf{U}_t)_j^n$ in Eq. (2.1) can be calculated by a local space-time flux balance over SE(j,n).

Similarly, $\mathbf{F}_j^n$ represents the numerical approximation to $\mathbf{F}$ at (x_j,t^n) evaluated with $\mathbf{U}=\mathbf{U}_j^n$. By using the chain rule, we also have

$$\begin{aligned}(\mathbf{F}_x)_j^n &= \mathbf{A}_j^n(\mathbf{U}_x)_j^n, \qquad (2.3)\\ (\mathbf{F}_t)_j^n &= \mathbf{A}_j^n(\mathbf{U}_t)_j^n, \qquad (2.4)\end{aligned}$$

where $\mathbf{A}=\partial\mathbf{F}/\partial\mathbf{U}$ is the Jacobian matrix, and it is a function of $\mathbf{U}$. Thus, $\mathbf{A}_j^n$ is $\mathbf{A}$ evaluated with $\mathbf{U}=\mathbf{U}_j^n$. Once $\mathbf{U}_j^n$ and $(\mathbf{U}_x)_j^n$ are obtained, all other variables can be expressed in terms of them.

2.2 The Method of Rhombic Elements

In this method, the space-time rhombic regions are taken as the solution elements. With the known values of $\mathbf{U}_{j\pm1/2}^{n-1/2}$ and $(\mathbf{U}_x)_{j\pm1/2}^{n-1/2}$, the task here is to march the solution to the mesh point (x_j,t^n). Refer to Fig. 2.3.

As a preliminary, recall that for any (j,n), $(\mathbf{U}_t)_j^n$ must be calculated so that we can use the Taylor expansions, Eqs. (2,1) and (2.2), for the space-time discretization. To this end, we impose the space-time flux balance over the rhombic region CE(j,n), i.e.,

$$\oint_{S(\mathrm{CE}(j,n))} \vec{\mathbf{h}}_m^* \cdot d\vec{s} = \int_{\mathrm{CE}(j,n)} p_m^* dR, \quad m=1,2,\ldots,M, \qquad (2.5)$$

where $\vec{\mathbf{h}}_m^*$ is the space-time flux vector, i.e,

$$\vec{\mathbf{h}}_m^* = (f_m^*, u_m^*), \quad m=1,2,\ldots,M, \qquad (2.6)$$

with u_m^* and f_m^* being the mth component of $\mathbf{U}^*$ and $\mathbf{F}^*$, respectively, as defined in Eqs. (2.1) and (2.2). In addition, p_m^* is the mth components of $\mathbf{P}^*$, which is a function of $\mathbf{U}$, evaluated with $\mathbf{U}=\mathbf{U}^*$. Henceforth, the components of the column vectors $\mathbf{U}_j^n$, $(\mathbf{U}_x)_j^n$, $(\mathbf{U}_t)_j^n$, $\mathbf{F}_j^n$, $(\mathbf{F}_x)_j^n$, and $(\mathbf{F}_t)_j^n$ are denoted by $(u_m)_j^n$, $(u_{mx})_j^n$, $(u_{mt})_j^n$, $(f_m)_j^n$, $(f_{mx})_j^n$, and $(f_{mt})_j^n$, for $m=1,2,\ldots,M$, respectively. Note that CE(j,n) here coincides with SE(j,n).

To proceed, we apply Gauss' divergence theorem to Eq. (2.5), and we get

$$\int_{\mathrm{CE}(j,n)} \left(\vec{\nabla}\cdot\vec{\mathbf{h}}_m^* - p_m^*\right) dR = 0. \qquad (2.7)$$

Substitute the definition of $\vec{\mathbf{h}}_m^*$, i.e., Eq. (2.6), into Eq. (2.7), and we get

$$\int_{\mathrm{CE}(j,n)} \left[(f_{mx})_j^n + (u_{mt})_j^n - p_m^* \right] dR = 0. \quad (2.8)$$

In addition, let

$$\bar{p}_{mj}^{*\,n} = \int_{\mathrm{CE}(j,n)} p_m^* dR / \diamond, \quad (2.9)$$

with

$$\diamond = \int_{\mathrm{CE}(j,n)} dR \quad (2.10)$$

being the space-time volume of $\mathrm{CE}(j,n)$. For the current uniform space-time mesh, this volume is independent of (j,n). As a result of Eqs. (2.9) and (2.10), Eq. (2.8) can be written as

$$\left[(f_{mx})_j^n + (u_{mt})_j^n - (\bar{p}_m^*)_j^n \right] \diamond = 0, \quad (2.11)$$

or

$$(f_{mx})_j^n + (u_{mt})_j^n - (\bar{p}_m^*)_j^n = 0. \quad (2.12)$$

We shall further assume that p_m^* is linear in x and t within $\mathrm{SE}(j,n)$. Then because the mesh point (j,n) is the center of $\mathrm{SE}(j,n)$, $(\bar{p}_m^*)_j^n = (p_m)_j^n$ where $(p_m)_j^n$ is the mth component of $\mathbf{P}$ evaluated with $\mathbf{U} = \mathbf{U}_j^n$. As a result, Eq. (2.12) reduces to

$$(f_{mx})_j^n + (u_{mt})_j^n - (p_m)_j^n = 0. \quad (2.13)$$

Note that, with the aid of Eq. (2.3), $(f_{mx})_j^n$ can be determined in terms of $(u_m)_j^n$ and $(u_{mx})_j^n$, for $m = 1, 2, \ldots, M$. As a result, $(u_{mt})_j^n$ can also be determined by $(u_m)_j^n$ and $(u_{mx})_j^n$ using Eq. (2.13). Therefore, the distributions of $\mathbf{U}^*$ and $\mathbf{F}^*$ inside $\mathrm{SE}(j,n)$ are determined by the independent unknowns $\mathbf{U}_j^n$, and $(\mathbf{U}_x)_j^n$ through the Taylor expansions Eqs. (2.1) and (2.2).

From the above discussions, the distributions of $\mathbf{U}$ and $\mathbf{F}$ are determined in $\mathrm{SE}(j \pm 1/2, n - 1/2)$, and we are ready to calculate $\mathbf{U}_j^n$ and $(\mathbf{U}_x)_j^n$ at the new time level. Refer to Fig. 2.3. For the interface between $\mathrm{CE}(j,n)$ and $\mathrm{CE}(j - 1/2, n - 1/2)$, we assume that the total space-time flux leaving $\mathrm{CE}(j - 1/2, n - 1/2)$ through $\overline{B'C'}$ is equal to the total space-time flux entering $\mathrm{CE}(j,n)$ through $\overline{CB}$. Note that $\vec{\mathbf{h}}_m^*$ along $\overline{CB}$ and $\overline{B'C'}$ are evaluated using information from $\mathrm{SE}(j,n)$ and $\mathrm{SE}(j - 1/2, n - 1/2)$, respectively. Thus, the above flux balance condition can be expressed as

$$\int_{\overline{B'C'}} \vec{\mathbf{h}}_m^* \cdot d\vec{s} + \int_{\overline{CB}} \vec{\mathbf{h}}_m^* \cdot d\vec{s} = \mathbf{0}. \quad (2.14)$$

Here $d\vec{s}$ in the first (second) integral in Eq. (2.14) points in the outward normal direction relative to $\mathrm{CE}(j - 1/2, n - 1/2)$ ($\mathrm{CE}(j,n)$). Similarly, the flux balance across the interface between $\mathrm{CE}(j,n)$ and $\mathrm{CE}(j + 1/2, n - 1/2)$ (refer to Fig. 2.3) can be expressed as

$$\int_{\overline{C''D''}} \vec{\mathbf{h}}_m^* \cdot d\vec{s} + \int_{\overline{DC}} \vec{\mathbf{h}}_m^* \cdot d\vec{s} = \mathbf{0}. \quad (2.15)$$

Again, $d\vec{s}$ in the first (second) integral in Eq. (2.15) points in the outward normal direction relative to $\mathrm{CE}(j + 1/2, n - 1/2)$ ($\mathrm{CE}(j,n)$).

By using Eq. (2.5) in conjunction with Eq. (1.10), integrals in Eqs. (2.14) and (2.15) can be expressed as,

$$\int_{\overline{B'C'}} \vec{\mathbf{h}}_m^* \cdot d\vec{s} = -\int_{B'}^{A'} f_m^* dt + \int_{A'}^{C'} u_m^* dx + \frac{\diamond}{4} (p_m)_{j-1/2}^{n-1/2}, \quad (2.16)$$

$$\int_{\overline{CB}} \vec{\mathbf{h}}_m^* \cdot d\vec{s} = -\int_{C}^{A} f_m^* dt + \int_{A}^{B} u_m^* dx + \frac{\diamond}{4} (p_m)_j^n, \quad (2.17)$$

$$\int_{\overline{C''D''}} \vec{\mathbf{h}}_m^* \cdot d\vec{s} = -\int_{A''}^{D''} f_m^* dt + \int_{C''}^{A''} u_m^* dx + \frac{\diamond}{4} (p_m)_{j+1/2}^{n-1/2}, \quad (2.18)$$

$$\int_{\overline{DC}} \vec{\mathbf{h}}_m^* \cdot d\vec{s} = -\int_{A}^{C} f_m^* dt + \int_{D}^{A} u_m^* dx + \frac{\diamond}{4} (p_m)_j^n. \quad (2.19)$$

These four equalities, Eqs. (2.16-19), can be easily verified by the space-time flux balance over $\triangle A'C'B'$, $\triangle ABC$, $\triangle A''D''C''$, and $\triangle ACD$, respectively. Note that, the integration over each triangle along the constant t and constant x based on the normal vector outward normal to the space-time region of interest has been changed into a line integration in the counterclockwise direction. Refer to Eq. (1.10). In addition, since a linear distribution of p_m^* in x and

t in each SE is assumed and a uniform mesh is used, the integration of p_m^* over each triangle in Eqs. (2.16) to (2.19) is equal to the corresponding nodal value of p_m multiplied by a quarter of the $\diamond$.

Substitute Eqs. (2.16-19) into Eqs. (2.14-15), and the above space-time flux balance over the oblique interfaces can be illustrated as space-time flux conservation over two square CEs, denoted by $\mathrm{CE}_-(j,n)$ and $\mathrm{CE}_+(j,n)$, i.e.,

$$\oint_{S(CE_-)} \vec{\mathrm{h}}_m^* \cdot d\vec{s} = \frac{\diamond}{4}\left((p_m)_{j-1/2}^{n-1/2} + (p_m)_j^n\right), \quad (2.20)$$

$$\oint_{S(CE_+)} \vec{\mathrm{h}}_m^* \cdot d\vec{s} = \frac{\diamond}{4}\left((p_m)_{j+1/2}^{n-1/2} + (p_m)_j^n\right). \quad (2.21)$$

Note that $\mathrm{CE}_-(j,n)$ is the union of $\triangle A'C'B'$ and $\triangle ABC$, and $\mathrm{CE}_+(j,n)$ is the union of $\triangle A"D"C"$ and $\triangle ACD$. Refer to Fig. 2.3. Note that Eqs. (2.20-21) here is a straightforward extension of the original CE/SE scheme as shown in [6] by adding the source term effects.

Equation (2.20) leads to M relations involving the independent unknowns U_j^n, $(\mathrm{U}_x)_j^n$, $\mathrm{U}_{j-1/2}^{n-1/2}$, and $(\mathrm{U}_x)_{j-1/2}^{n-1/2}$, and Eq. (2.20) leads to the other M relations involving U_j^n, $(\mathrm{U}_x)_j^n$, $\mathrm{U}_{j+1/2}^{n-1/2}$, and $(\mathrm{U}_x)_{j+1/2}^{n-1/2}$. With the flow properties at the mesh points $(j-1/2, n-1/2)$ and $(j+1/2, n-1/2)$ known, the $2M$ components of U_j^n and $(\mathrm{U}_x)_j^n$ can be determined by the above $2M$ relations.

Note that $(p_m)_j^n$ in Eqs. (2.19) and (2.20) is a function of $(u_m)_j^n$. Therefore, Eqs. (2.20) and (2.21) are implicit equations in terms of U_j^n and $(\mathrm{U}_x)_j^n$. To solve these equations, Newton's method is used. Usually, two or three Newton's steps are needed for a satisfactory convergence.

The method of rhombic elements is useful for treating the conservation laws with non-stiff source terms. However, when the source terms become stiff the method would fail. With stiff source terms, the dominant effect in the the overall flux balance, i.e., Eqs. (2.20) and (2.21), is due to the source-term effects. In particular, the stiff source terms would directly impact the calculation of (i) temporal derivatives $(u_{mt})_{j\pm1/2}^{n-1/2}$ (refer to Eq. (2.13)), and (ii) the space-time area integration of the source terms (refer to Eqs. (2.16-19)). As such, any small difference between the values of $(u_m)_{j-1/2}^{n-1/2}$ and $(u_m)_{j+1/2}^{n-1/2}$ (and/or small differences between $(u_{mx})_{j-1/2}^{n-1/2}$ and $(u_{mx})_{j+1/2}^{n-1/2}$) will be amplified by the stiffness factor. As a result, huge differences occur between $(u_{mt})_{j-1/2}^{n-1/2}$ and $(u_{mt})_{j+1/2}^{n-1/2}$, and between $(p_m)_{j-1/2}^{n-1/2}$ and $(p_m)_{j+1/2}^{n-1/2}$ when solving Eqs. (2.20) and (2.21). Here, we conjecture that the numerical calculation for $(u_m)_j^n$ and $(u_{mx})_j^n$ governed by Eqs. (2.20) and (2.21) at the new time step could be contaminated by the round-off errors. As will be shown in the section of numerical examples, the iterative procedure in Newton's method would fail in solving these stiff relaxation systems.

2.3 The Method of Rectangular Elements

In light of the above difficulty with the method of rhombic elements, we conjecture that the remedy for treating the stiff source terms is to avoid the above discussed amplification effects. To this end, we propose to re-distribute the space-time regions such that all source-term effects are hinged on the mesh node (x_j, t^n) at the new time level.

As shown in Fig. 2.4, the relative locations of three SEs for the space-time method is identical to that in the method of rhombic elements. The CEs and SEs, however, have taken the shape of a rectangular area, with a magnitude equal to $\Delta x \Delta t/2$, and a line segment sticking out on the top of the rectangle. Henceforth, we refer to this new extension of the CE/SE method as the method of rectangular elements.

In this new construction, we impose the same flux balance conditions as that in the method

of rhombic elements, i.e., Eqs. (2.20) and (2.21). Refer to Fig. 2.4. Here, however, the calculation is different from the method of rhombic elements in the following two aspects: (i) with the known values of $(u_m)_{j\pm1/2}^{n-1/2}$ and $(u_{mx})_{j\pm1/2}^{n-1/2}$, the calculation of $(u_{mt})_{j\pm1/2}^{n-1/2}$ is simply by using

$$(u_{mt})_{j\pm1/2}^{n-1/2} + (f_{mx})_{j\pm1/2}^{n-1/2} = 0. \qquad (2.22)$$

As a contrast to that in the method of rhombic elements, Eq. (2.13), no source term effect is included here. Note that this temporal derivatives are used only along the line segment sticking out on the top of the rectangular elements. By adopting the nomenclature of computational reactive flows, a frozen model, i.e., convection equations without chemical reactions, is used here for the time marching scheme. (ii) In the calculation of the overall flux balance over $CE_{\pm}$, i.e., Eqs. (2.20) and (2.21), the integration of the source term over the space-time regions is calculated totally based on the flow properties at (x_j, t^n), i.e.,

$$\oint_{S(CE_-)} \vec{h}_m^* \cdot d\vec{s} = \frac{\Delta x \Delta t}{2}(p_m)_j^n, \qquad (2.23)$$

$$\oint_{S(CE_+)} \vec{h}_m^* \cdot d\vec{s} = \frac{\Delta x \Delta t}{2}(p_m)_j^n. \qquad (2.24)$$

This condition is clearly indicated by the shape of the new conservation elements. Based on these two modifications, one can change Eqs. (2.16)-(2.19) accordingly, and the final algebraic equations for the method of rectangular elements can be obtained. Similar to that in the method of rhombic elements, we have $2M$ equations for $2M$ unknowns and flow solution at the new time step can be determined. Similar to that in Eqs. (2.20) and (2.21), $(p_m)_j^n$ in Eqs. (2.23) and (2.24) is a function of $(u_m)_j^n$, and Eqs. (2.23) and (2.24) are implicit relations in terms of $(u_m)_j^n$ and $(u_{mx})_j^n$. Thus, Newton's method is used to solve the equation set.

As such, we numerically avoid the above-mentioned amplification effects because the flow properties and their gradients associated with the mesh nodes at $(x_{j-1/2}, t^{n-1/2})$ and $(x_{j+1/2}, t^{n-1/2})$ are not involved in the source-term calculations. However, the method of rectangular elements is just a numerical remedy for treating stiff source terms. For a faithful simulation to the physical phenomenon, one should resolve the time and space scales associated with the source terms. In this sense, the method of the rhombic elements is more fundamental, and the method of rectangular elements is ad hoc.

In addition, the lattice stencil associated with the method of the rhombic elements is symmetric in both x and t. Therefore, the method bears the same property of space-time inversion for isentropic flows as that in the original CE/SE method. For the method of rectangular elements, however, the mesh structure is asymmetric with respect to time, and the method can only march forward in time. In general, artificial damping has been added into the discrete system such that the numerical process here is irreversible. Nevertheless, since the union of all rectangular elements covers the whole space-time domain without overlapping, the source term effect in an integral sense satisfies the local and global space-time flux balance.

As an aside, the above approach using the rectangular elements can also be implemented by using a modern upwind scheme. Essentially, Eq. (1.6) can be employed and the calculation of the source term should be based on the integration of the source term over the rectangular space-time volume. If an explicit time marching scheme is used, all source term effect should be attributed to the mesh node at the new time step to avoid the amplification effect due to the stiff source term. In addition, since all the source term effects are treated based on the solution at the new time step, in calculating the interfacial fluxes, the Riemann solver should be based on the frozen model in the explicit time marching. To solve the final equations, a local implicit scheme can be constructed and Newton's method can be exploited.

3 Numerical Examples

3.1 Flow over a Nozzle

As the first and also the simplest test of the source term treatments in the present paper, we calculate a steady one-dimensional flow through a variable area duct, a standard test for shock capturing schemes proposed by Shubin et al. [40]. The governing equations are

$$\frac{\partial \mathbf{U}}{\partial t} + \frac{\partial \mathbf{F}}{\partial x} + \mathbf{H} = 0. \tag{3.1}$$

where

$$\mathbf{U} = \begin{pmatrix} \rho A \\ \rho u A \\ \rho E A \end{pmatrix}, \quad \mathbf{F} = \begin{pmatrix} \rho u A \\ (\rho u^2 + P)A \\ (\rho E + P)uA \end{pmatrix},$$
$$\mathbf{H} = \begin{pmatrix} 0 \\ P\frac{\partial A}{\partial x} \\ 0 \end{pmatrix}, \tag{3.2}$$

where ρ is the density, u is the velocity, E is the total energy, P is pressure, and A is the cross-section area of the nozzle. The source term is composed of the pressure multiplied by the gradient of the area change. The prescribed area is $A(x) = 1.398 + 0.347tanh(0.8 * x - 4.)$ with $0 \leq x \leq 10$. The specified inflow conditions are $A_{in} = 1.05$, $\rho_{in} = 0.502$, $e_{in} = 1.897$, $u_{in} = 1.299$, and the outflow conditions are $A_{out} = 1.745$, $\rho_{out} = 0.776$. The exact solution for the present problem is a normal shock stands at $A = 1.347$ ($x = 4.816$). The numerical solution of the density distribution is presented in Fig. 3.1. The result is obtained by the method of rhombic elements. Although not shown, the result obtained by using the method of rectangular elements is identical to that presented here. Three sets of mesh, with the numbers of grid nodes of 41 ,81, and 161, are used. As we refine the mesh, the numerical solution converges to the exact solution.

3.2 Model Scalar Equation by LeVeque and Yee

A model scalar equation was proposed by LeVeque and Yee [28] to study the source term treatment:

$$\frac{\partial u}{\partial t} + \frac{\partial u}{\partial x} = -\mu u(u-1)(u-0.5). \tag{3.3}$$

The source term is stiff for large μ. In [28], detailed discussion of the model equation is provided. In short, due to the source term, there are two equilibrium solutions at $u = 1$ and $u = 0$. And $u = 0.5$ is an unstable point. Whenever the solution deviates from the two equilibria, the source term will be activated and push the solution toward 1 if $u > 0.5$ and toward 0 if $u < 0.5$. In particular, the solution with piecewise constant initial data

$$u(x,0) = \begin{cases} 1 & \text{if } x < x_o \\ 0 & \text{if } x > x_o \end{cases} \tag{3.4}$$

is simply $u(x,t) = u(x-t,0)$.

Figure 3.2(a) shows the numerical solution of the model equation at $t = 0.6$ using the method of rhombic elements. The setup is identical to that in LeVeque an Yee's work. In all calculations, forty grid nodes are used. For $\mu \leq 200$, we obtained accurate solutions. For various μ, the solution is virtually identical and here we just plot the case of $\mu = 200$. For $\mu > 200$, Newton's method doesn't converge and we cannot obtain any solution.

When we apply the method of rectangular elements, however, we always get accurate solution. For $0.1 < \mu < 10^{16}$, the scheme produces identical solutions. In Fig. 3.2(b), the case of $\mu = 10^{16}$ is plotted. The solution in Fig. 3.2(b) is identical to that in Fig. 3.2(a).

It was pointed out by Huynh and Prashant [41] that in our solution there is always a node where $u = 0.5$. However, according to the analytical solution, $u = 0.5$ is unstable. This is because a linear distribution of the source term is used in our discretized equation. Refer to Eq. (2.13). As

a result, the source term, which is a cubic function of the unknown, was not well represented. Thus, Newton's method always overshoot, and the numerical solution converged to the middle value $u = 0.5$. In future, we shall investigate the space-time discretization for source term with complex functional form. Presumably, a careful calculation of $\bar{p}_m^*$ in Eq. (2.12) by taking into account of the actual function of the source term could improve this situation.

3.3 Shock Wave in a Constant-Temperature Bath

Pember [29] suggested a test case for the treatment of stiff source terms. Consider the one-dimensional Euler equations with a special heat transfer term in the energy equation:

$$\frac{\partial \mathbf{U}}{\partial t} + \frac{\partial \mathbf{F}}{\partial x} + \mathbf{H} = \mathbf{0} \tag{3.5}$$

where the flow properties $\mathbf{U}$ and the flux $\mathbf{F}$ are defined as usual, and the source term $\mathbf{H} = (0, 0, K\rho(T - T_o))^{\mathrm{T}}$. The function of the source term is to force a constant temperature T_o upon the whole flow field. The equilibrium counterpart of the relaxation system is

$$\frac{\partial \rho}{\partial t} + \frac{\partial \rho u}{\partial x} = 0, \tag{3.6}$$

$$\frac{\partial \rho u}{\partial t} + \frac{\partial \rho u^2 + p^*}{\partial x} = 0, \tag{3.7}$$

where the pressure $p^*(\rho) = (\gamma - 1)\rho e_o$, with e_o as the internal energy of the gas at $T = T_o$. Jin [33] also used this case as one of the numerical examples reported in his paper.

We conducted the calculation for x in [0,1] discretized by 201 grid nodes. The conductivity K in the flow system was set be to 10^8, 10^{12}, and 10^{16}. Essentially we get the same result for different K. Figure 3.3 shows flow properties at $t = 0.3$. The flow field is composed of a right-moving shock and a left-moving rarefaction wave. The relaxation time $\epsilon = 1/K$ is underresolved for all three cases. The numerical solution is almost identical as compared to that provided by Jin. Note that in the plot for temperature distribution, our solution is closer to the imposed constant temperature T_o.

3.4 The ZND Wave

The classical theory of Zeldovich, von Neumann, and Doring (ZND) of the one-dimensional detonation waves can be formulated using the Euler equations coupled with a species equation:

$$\frac{\partial \rho Z}{\partial t} + \frac{\partial \rho u Z}{\partial x} = -K\rho Z \exp\left(\frac{-E^+}{T}\right), \tag{3.8}$$

where Z is the reactant mass fraction. The source term of the species equation is composed of a single-step irreversible reaction formulated according to Arrhenius' law. For this reacting flows, the definition of the total energy E in the energy equation is modified to include the chemical energy $E = e + q_o Z + u^2/2$, where q_o is the chemical energy of the reactant. Previously, this set of equations has been thoroughly studied by Bourlioux et al. [38, 39] through stability analysis and CFD simulations.

The initial condition of the present calculation is a long tube filled with reactant with a piston on one end moving at a constant speed into the quiescent reactant. We use the piston face as the origin of the the coordinate system. According to this coordinate frame, reactant is charged into a closed-end tube at a constant speed. Thus, a shock wave is reflected on the closed end to ignite the reactant.

The parameters of the flow field in the present calculation are set as $q_o = 50$, $E^+ = 40$, $\gamma = 1.2$, and the over drive coefficient equal to 1.6. According to the classical theory for detonation instability, a transient but stable detonation wave should be obtained with these parameters. Figure 3.4 shows the distributions of pressure, density, and reactant mass fraction of a stable detonation wave. The detonation wave propagates from left to right and the flow field is composed of: (i) the quiescent state of the reactant before the shock, (ii) a von Neumann spike with finite

rate reaction, and (iii) the equilibrium state between the piston and the spike. The difference between the analytical solution and our solution is less than 5%. If we raised the activation energy of the chemical reaction E^+ to 50, the detonation wave became unstable and a longitudinal wave bouncing between the piston and the shock could be observed.

4 Concluding Remarks

In the present paper, we report the extension of the CE/SE method for solving convection equations with source terms. By treating space and time in a unified manner, the source terms are included as volumetric integral over space-time conservation elements such that it becomes an integral part of the overall space-time flux balance. In particular, the treatments of the source term can be visualized by the employed space-time geometries. Two conservation elements are considered: (i) rhombic elements, and (ii) the rectangular elements. Both treatments result in locally implicit equations in terms of flow properties at the new time level. Thus, Newton's method is used to solve the equations. The method of rhombic elements is a straightforward extension of the original CE/SE scheme and is suitable for the non-stiff source terms. This method would fail when it is used to solve stiff relaxation systems. We conjecture that the failure is due to an amplification effects by the stiff source terms over the differences of the flow properties at adjacent nodes in the same time level. The method of rectangular elements eliminates these amplification effects by a re-distribution of the space-time region such that the source-term effects are hinged on the mesh nodes at new time level. As a result, the method is robust and stable for treating under-resolved stiff source terms. The above finding was supported by the numerical examples reported in the paper.

5 Acknowledgments

The first author of the present paper wants to thank Dr. A. Bourlioux of CERCA and University of Montreal for providing the analytical solution solver of the ZND wave. The first author also wants to thank Dr. Robert Stubbs of NASA Lewis Research Center for the financial support of this research project.

References

[1] S.C. Chang and W.M. To, "A New Numerical Framework for Solving Conservation Laws – The Method of Space-Time Conservation Element and Solution Element," NASA TM 104495, August 1991.

[2] S.C. Chang, "On an Origin of Numerical Diffusion: Violation of Invariance Under Space-Time Inversion", Proceedings of the 23rd Modeling and Simulation Conference, April 1992, Pittsburgh, PA, William G. Vogt and Marlin H. Mickle eds., Part 5, pp. 2727-2738. Also published as NASA TM 105776.

[3] S.C. Chang and W.M. To, "A Brief Description of a New Numerical Framework for Solving Conservation Laws – The Method of Space-Time Conservation Element and Solution Element", Proceedings of the 13th International Conference on Numerical Methods in Fluid Dynamics, July 6-10, 1992, Rome, Italy, M. Napolitano and F. Sabetta, eds. Also published as NASA TM 105757.

[4] S.C. Chang, "New Developments in the Method of Space-Time Conservation Element and Solution Element – Applications to the Euler and Navier-Stokes Equations", Presented at the Second U.S. National Congress on Computational Mechanics, August 16-18, 1993, Washington D.C. Published as NASA TM 106226.

[5] S.C. Chang, X.Y. Wang and C.Y. Chow, "New Developments in the Method of

Space-Time Conservation Element and Solution Element – Applications to Two-Dimensional Time-Marching Problems", NASA TM 106758, December 1994.

[6] S.C. Chang, *J. Comput. Phys.*, **119**, (1995) pp. 295-324.

[7] S.C. Chang, X.Y. Wang and C.Y. Chow, "The Method of Space-Time Conservation Element and Solution Element – Applications to One-Dimensional and Two-Dimensional Time-Marching Flow Problems", AIAA Paper 95-1754, the 12th AIAA CFD Conference, June 1995, San Diego, CA. Also published as NASA TM 106915.

[8] S.C. Chang, X.Y. Wang, C.Y. Chow and A. Himansu, "The Method of Space-Time Conservation Element and Solution Element – Development of a New Implicit Solver", the Ninth International Conference on Numerical Methods in Laminar and Turbulent Flow, July 1995, Atlanta, GA. Also published as NASA TM 106897.

[9] S.C. Chang, C.Y. Loh and S.T. Yu, "Computational Aeroacoustics via a New Global Conservation Scheme," the 15th International Conference on Numerical Methods in Fluid Dynamics, June 1996, Monterey, CA.

[10] S.C. Chang, S.T. Yu, A. Himansu, X.Y. Wang, and C.Y. Loh, "The Method of Space-Time Conservation Element and Solution Element – A New Paradigm for Numerical Solution of Conservation Laws," to appear in *Computational Fluid Dynamics Review 1996*, Edited by M.M. Hafez and K. Oshima, John Wiley and Sons, West Sussex, UK.

[11] C.Y. Loh, S.C. Chang, J.R. Scott and S.T. Yu, "Application of the Method of Space-Time Conservation Element and Solution Element to Aeroacoustics Problems," the 6th International Symposium of CFD, September 1995, Lake Tahoe, NV.

[12] C.Y. Loh, S.C. Chang, J.R. Scott and S.T. Yu, "The Space-Time Conservation Element Method – A New Numerical Scheme for Computational Aeroacoustics," AIAA Paper 96-0276, the 34th AIAA Aerospace Sciences Meeting, January 1996, Reno, NV.

[13] C.Y. Loh, S.C. Chang and J.R. Scott, "Computational Aeroacoustics via the Space-Time Conservation Element / Solution Element Method," AIAA Paper 96-1687, the 2nd AIAA/CEAS Aeroacoustics Conference, May 1996, State College, PA.

[14] X.Y. Wang, C.Y. Chow and S.C. Chang, "Application of the Space-Time Conservation Element and Solution Element Method to Shock-Tube Problem," NASA TM 106806, December 1994.

[15] X.Y. Wang, "Computational Fluid Dynamics Based on the Method of Space-Time Conservation Element and Solution Element," Ph.D. Dissertation, 1995, Department of Aerospace Engineering, University of Colorado, Boulder, CO.

[16] X.Y. Wang, C.Y. Chow and S.C. Chang, "Application of the Space-Time Conservation Element and Solution Element Method to Two-Dimensional Advection-Diffusion Problems," NASA TM 106946, June 1995.

[17] X.Y. Wang, C.Y. Chow and S.C. Chang, "High Resolution Euler Solvers Based on the Space-Time Conservation Element and Solution Element Method," AIAA Paper 96-0764, the 34th AIAA Aerospace Sciences Meeting, January 1996, Reno, NV.

[18] X.Y. Wang, C.Y. Chow and S.C. Chang, "Numerical Simulation of Flows Caused by Shock-Body Interaction," AIAA Paper 96-2004, the 27th AIAA Fluid Dynamics Conference, June 1996, New Orleans, LA.

[19] X.Y. Wang, C.Y. Chow and S.C. Chang, "An Euler Solver Based on the Method of Space-Time Conservation Element and Solution Element," the 15th International Conference on Numerical Methods in Fluid Dynamics, June 1996, Monterey, CA.

[20] J.R. Scott and S.C. Chang, "A New Flux Conserving Newton's Method Scheme for the Two-Dimensional, Steady Navier-Stokes Equations," NASA TM 106160, June 1993.

[21] J.R. Scott, "A New Flux-Conserving Numerical Scheme for the Steady, Incompressible Navier-Stokes Equations," NASA TM 106520, April 1994.

[22] J. R. Scott and S.C. Chang, *Comp. Fluid Dyn.*, Vol. **5** (1995) pp. 189-212.

[23] J.R. Scott and S.C. Chang, "The Space-Time Solution Element Method – A New Numerical Approach for the Navier-Stokes Equations," AIAA Paper 95-0763, the 33rd AIAA Aerospace Sciences Meeting, January 1995, Reno, NV.

[24] J. R. Scott, "Further Development of a New, Flux-Conserving Newton Scheme for the Navier-Stokes Equations," NASA TM 107190, March 1996.

[25] H.F. Davis and A.D. Snider, "Introduction to Vector Analysis," 6th Ed., Wm. C. Brown Publishers, Dubuque IA (1991) pp. 274-281.

[26] M. Vinokur, *J. Comput. Phys.*, **81**, pp. 1-52 (1989).

[27] P. Colella, A. Majda, and V. Roytburd, *SIAM J. Sci. Stat. Comput.*, **7**, 4 (1986) pp. 1059-1080.

[28] R.J. LeVeque and H.C. Yee, *J. Comput. Phys.*, **86** (1990) pp. 187-210.

[29] R.B. Pember, *SIAM J. Appl. Math.*, **53**, 5 (1993) pp. 1293-1330.

[30] R.B. Pember, *SIAM J. Sci. Comput*, **14**, 4 (1993) pp. 824-859.

[31] T.P. Liu, *Commun. Math. Phys.*, **108**, pp. 153 (1987).

[32] G.B. Whitham, *Linear and Nonlinear Waves*, (Wiley, New York, 1974).

[33] S. Jin, *J. Comput. Phys.*, **122** (1995) pp. 51-67.

[34] P.L. Roe and M. Arora, *Numer. Methods for Partial Diff. Equations*, **9** (1993) pp.459-505.

[35] M. Arora, "Explicit Characteristic-Based High-Resolution Algorithms for Hyperbolic Conservation Laws with Stiff Source Terms," Ph.D. dissertation, Aerospace Engineering and Scientific Computing, University Michigan (1996).

[36] J. Bell, P. Colella, J. Trangenstein, and M. Welcome, "Adaptive Methods for High Mach Number Reacting Flows," AIAA Paper 87-1168, the 8th AIAA CFD Conference, Honolulu, HI, June 1987.

[37] E. Harabetian, *J. Comput. Phys.*, **103** (1992) pp.350-358.

[38] A. Bourlioux and A.J. Majda, V. Roytburd, *SIAM J. Appl. Math.*, **51**, 2 (1991) pp.303-343.

[39] A. Bourlioux and A.J. Majda, *Phil. Trans. R. Soc. Lond. A*, **350** (1995) pp. 29-68.

[40] G.R. Shubin, A.B. Stephens, and H.M. Glaz, *J. Comput. Phys.*, **39** (1981) pp. 364-374.

[41] H.T. Huynh and P. Prashant, NASA Lewis Resaerch Center, Ohio and Coastal Carolina University, South Carolina, private communication.

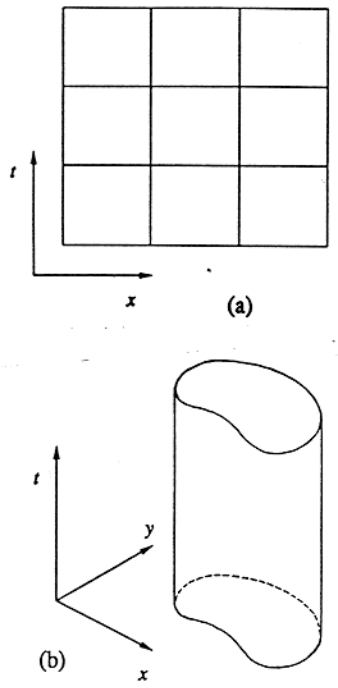

Fig. 1.1 Space-time conservation elements for methods using a fixed spatial domain: (a) one spatial dimension, and (b) two spatial dimensions.

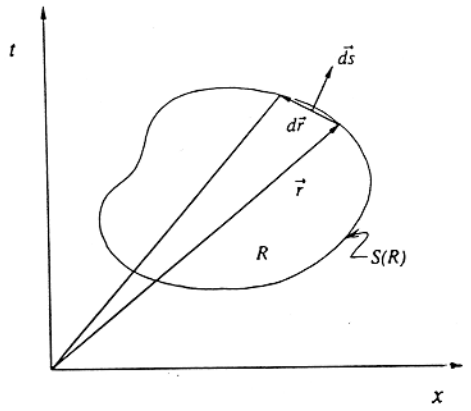

Fig. 1.2 A space-time conservation element with an arbitray space-time domain in one spatial domain.

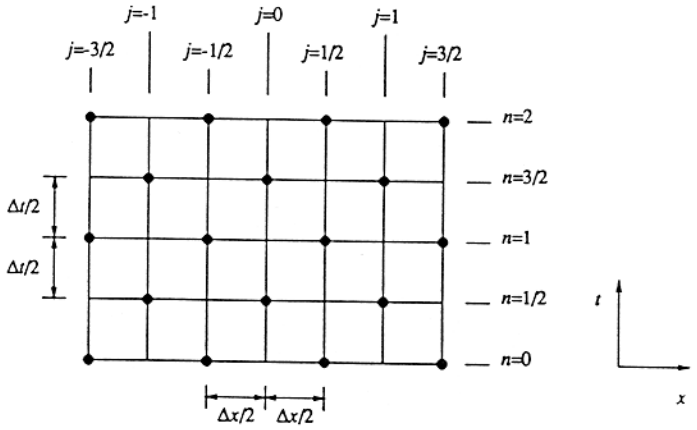

Fig. 2.1 The space-time mesh of the CE/SE method.

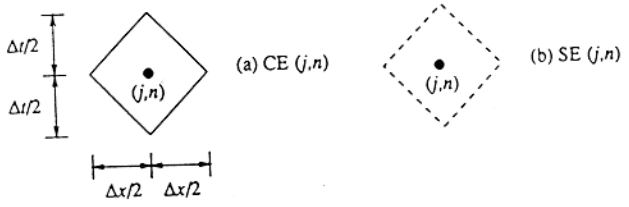

Fig. 2.2 A CE(j,n) and an SE(j,n) of the method of rhombic elements for the mesh point (j,n).

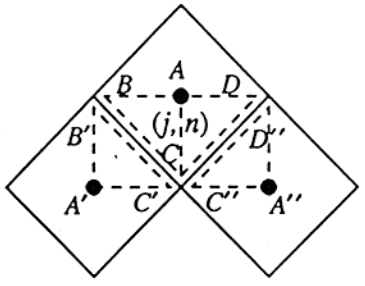

Fig. 2.3 The neighboring CEs (SEs) in the method of rhombic elements.

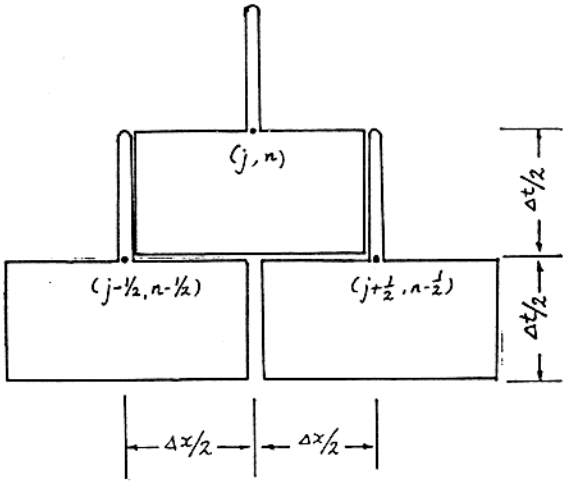

Fig. 2.4 The neighboring CEs (SEs) in the method of rectangular elements.

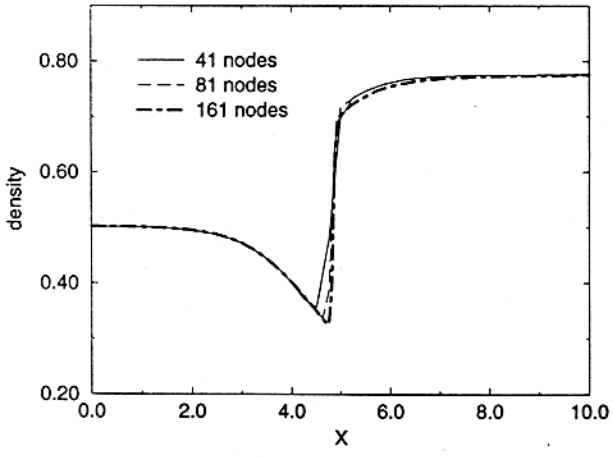

Fig. 3.1 The density distributions over a nozzle proposed by Shubin et al. [40].

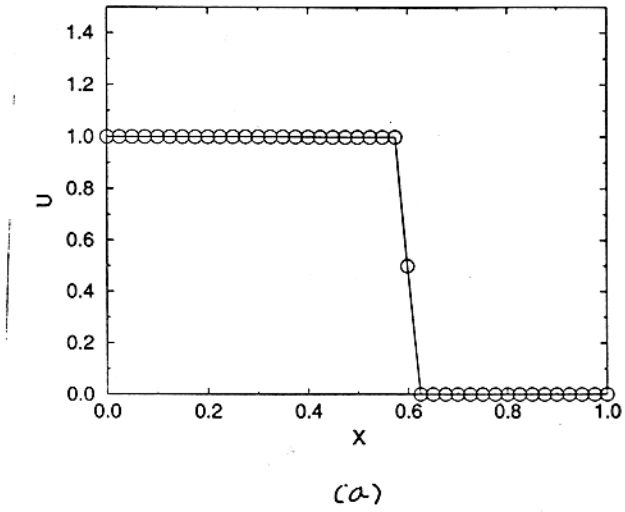

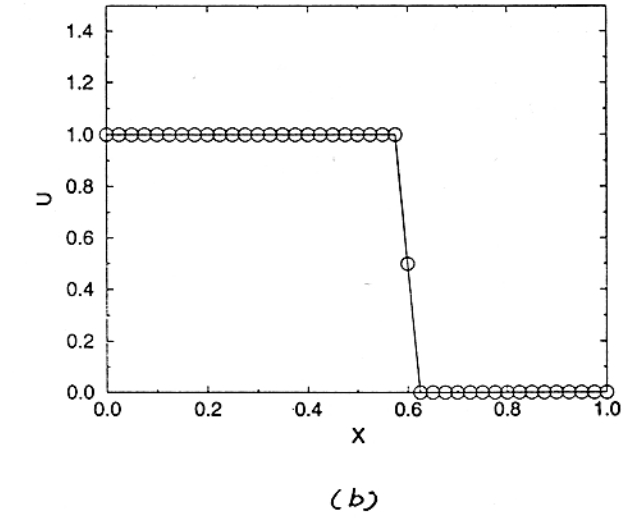

Fig. 3.2 The solution of a model scalar equation proposed by Leveque and Yee [28]: (a) by the method of rhombic elements for $\mu < 200$, and (b) by the method of rectangular elements for $\mu < 10^{16}$.

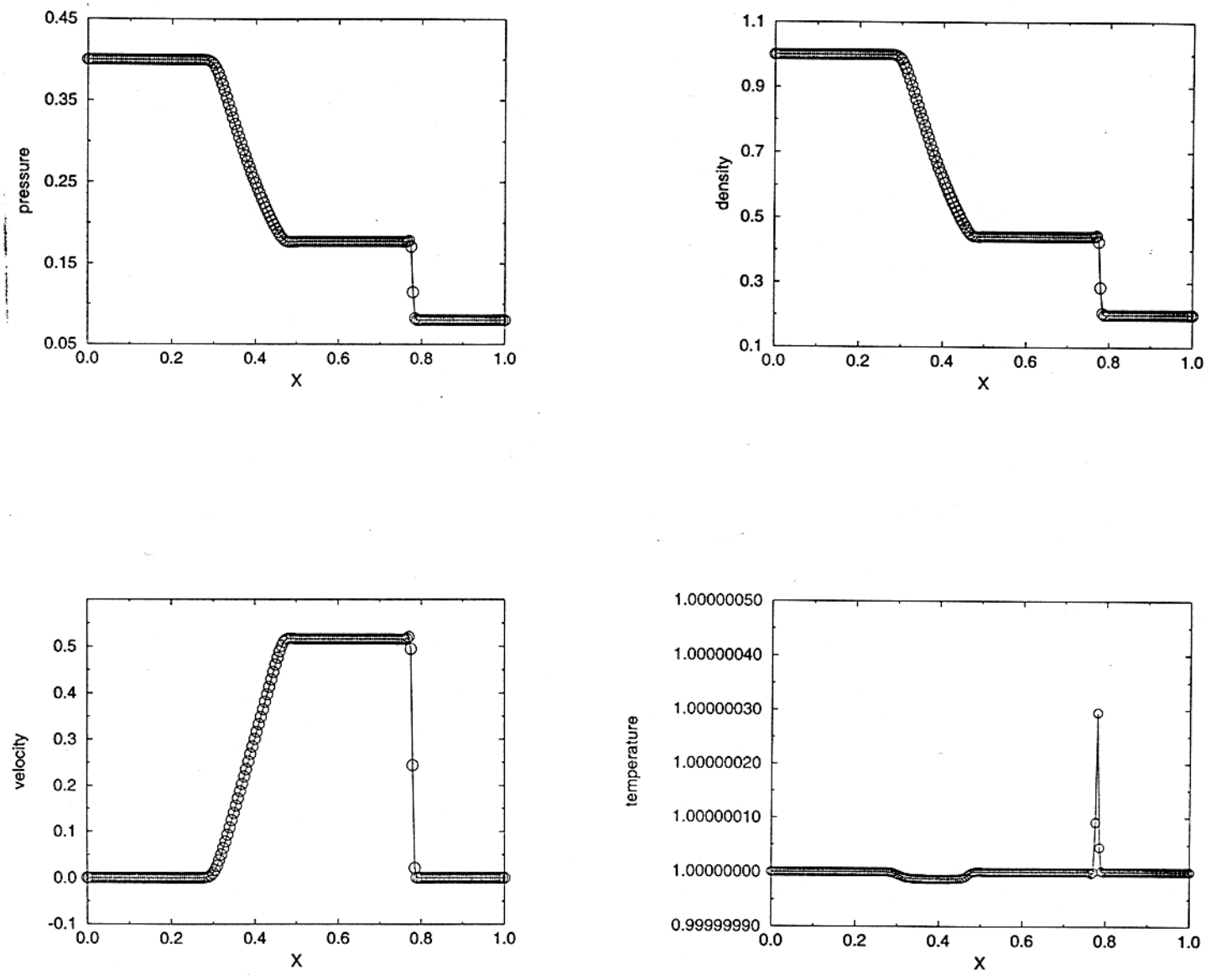

Fig. 3.3 The flow solution of a shock tube in a constant temperature bath at $t = 0.3$: (a) pressure, (b) density, (c) veloicty, and (d)temperaure.

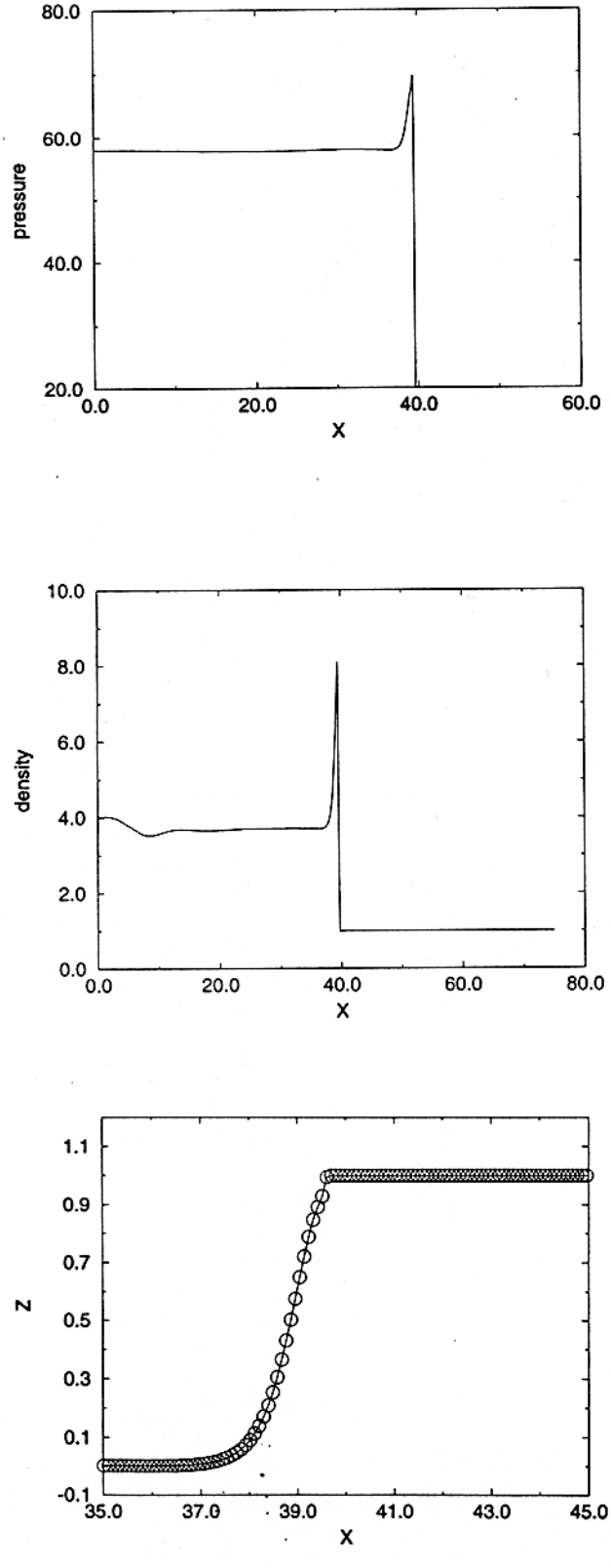

Fig. 3.4 The distributions of (a) pressure, (b) density, and (c) reactant mass fraction of a ZND wave.